DEVELOPMENT OF ITER RELEVANT ICRF WALL CONDITIONING TECHNIQUE ON EUROPEAN TOKAMAKS

A.Lyssoivan[1], R.Koch[1], D.Van Eester[1], M.Vervier[1], R.Weynants[1], H.G.Esser[2], V.Philipps[2], E.Gauthier[3], D.A.Hartmann[4], J.-M.Noterdaeme[4,5], V.Bobkov[4], F.Braun[4], I.Monakhov[6], A.Walden[6], TEXTOR Team, TORE SUPRA Team, ASDEX Upgrade Team and JET EFDA Contributors

[1] LPP-ERM/KMS, Association EURATOM-BELGIAN STATE, 1000 Brussels, Belgium*;
[2] Institut fьr Plasmaphysik FZ Jьlich, EURATOM Association, D-52425 Jьlich, Germany*;
[3] Association EURATOM-CEA, DSM-DRFC, CEA Cadarache, 13108 St Paul lez Durance, France
[4] Max-Planck Institut fьr Plasmaphysik, EURATOM Association, D-85748 Garching, Germany;
[5] Gent University, EESA Department, B-9000 Gent, Belgium;
[6] Association EURATOM-UKAEA, Culham Science Centre, Abingdon OX14 3DB, UK

In future reactor-scale superconducting fusion devices such as ITER, the presence of a permanent high magnetic field will prevent the use of conventional Glow Discharge Conditioning in between shots. Therefore, only discharges fully compatible with the presence of high magnetic field can be used for the conditioning procedure. ICRF discharge has a high potential to solve this problem. The paper presents a review of the new ICRF wall conditioning technique developed on limiter tokamaks TEXTOR and TORE SUPRA and the results of the first tests on the divertor tokamaks ASDEX Upgrade and JET.
PACS: 52.25.Jm, 52.35.Hr, 52.40.Fd, 52.40.Hf, 52.50.Qt

1. INTRODUCTION

First wall conditioning is considered as an indispensable tool to control particle recycling and to reduce plasma impurities and tritium inventory in the plasma facing components of future superconducting fusion reactors like ITER. The presence of permanent high magnetic field in such machines will prevent the use of conventional Glow Discharge Conditioning (G-DC) in between shots due to short-circuit occurring between anode and cathode along the magnetic field lines. Therefore, only discharges fully compatible with the presence of high magnetic field can be used for the conditioning procedure. Discharge conditioning with waves in the Ion Cyclotron Range of Frequencies (ICRF-DC) is considered as a promising candidate for solving the mentioned problems. Originally developed for routine use in stellarators for the target plasma production ($\omega < \omega_{ci}$) [1] and wall conditioning ($\omega >> \omega_{ci}$) [2], ICRF-DC in the frequency range $\omega > \omega_{ci}$ was successfully tested later on the limiter tokamaks (without divertor) TEXTOR [3-5], TORE SUPRA [6-8] and HT-7 [9]. The present generation of ICRF antennas with poloidal RF current were used in those experiments without any modifications in hardware. The encouraging efficiency of wall conditioning achieved with ICRF-DC on circular tokamaks stimulated next steps in the development of the ITER relevant ICRF wall conditioning technique. The first ICRF-DC experiments in large-size non-circular divertor tokamaks have been performed on ASDEX Upgrade (AUG) and JET [10]. In this paper, a review of the ICRF-DC studies on the present-day European tokamaks is presented and a perspective on the application of the new technique in ITER is discussed.

2. PRINCIPLES OF ICRF PLASMA PRODUCTION BY POLOIDAL ANTENNA

The initiation of ICRF discharge in a toroidal magnetic field B_T results from the absorption of RF energy mainly by electrons [11,12]. The RF $\tilde{E}_z$-field (parallel to the B_T-field) is thought to be responsible for this process. However, in the ICRF band for the present-day fusion devices (~10–100 MHz), for most of the antenna κ_z-spectrum, the RF waves cannot propagate in the vacuum vessel: $\kappa_\perp^2 = \omega^2/c^2 - \kappa_z^2 < 0$, where $\kappa_\perp$ is the perpendicular wave-vector, $\omega = 2\pi f$, f is the RF generator frequency. Hence, the neutral gas breakdown and initial ionization may only occur locally at the antenna-near $\tilde{E}_z$-field (evanescent in vacuum). In the general case of a poloidal loop-type ICRF antenna with a tilted Faraday shield (FS), the RF $\tilde{E}_z$-field in vacuum can be induced *electrostatically* and *inductively* [4]. The electrostatic mechanism results from the RF potential difference between the central conductor and the side parts of the antenna box (side protection RF limiters):

$$\tilde{E}_{z-es}(r) \approx (\tilde{U}_{RF}/l_{z1})\exp(-\kappa_{z1}r) \ , \quad (1)$$

where $\tilde{U}_{RF}$ is the maximum RF voltage on the current strap, l_{z1} is the gap between the current strap and the antenna box, $\kappa_{z1} = 2\pi/l_{z1}$, r is the radial distance away from the antenna strap. The inductive mechanism results from the RF voltage induced between the FS rods by the time-varying magnetic flux:

$$\tilde{E}_{z-em}(r) \approx (\tilde{U}_{RF}/l_\theta N)\sin(\beta \pm \gamma)\exp(-\kappa_{z2}r) \ . \quad (2)$$

Here N is the number of FS slots, l_θ is the width of FS slots, l_{z2} is the FS width, $\kappa_{z2} = 2\pi/l_{z2}$. It is clear seen from Eq.(2), that both tilted FS (angle β) and vertical ripples of the B_T-field (angle γ) can contribute to the generation of this component of RF field in the antenna vicinity. Such a simplified analytical description of the antenna-near $\tilde{E}_z$-field in vacuum was found in a good agreement with numerical simulations done for the real antenna configurations using the 3D electromagnetic codes [4].

An analysis of the parallel equation of motion for electrons in terms of the Mathieu equation [11] revealed that electrons perform complex motions: linear fast oscillations under the action of the Lorentz force and non-linear slow motions under the action of the RF ponderomotive force. Energy can be transferred to the electrons only through random collisions with gas molecules, atoms or ions. If the oscillation energy of electrons exceeds the ionization potential for molecules $m_e v_{ez}^2/2 \geq \varepsilon_i$, the gas ionization can proceed. However, if

*Partners in the Trilateral Euregio Cluster (TEC)

 Problems of Atomic Science and Technology. 2005. № 1. Series: Plasma Physics (10). P. 44-48

the ponderomotive force expels electrons out of the antenna region on a time-scale of the order of the RF period, the ionization process is hampered. This will happen when the stability parameter for the Mathieu equation $\varepsilon = e\tilde{E}_z / m_e\omega^2 L_z$ meets the condition for unstable solutions: $\varepsilon \geq 1/4 - 2\varepsilon^2$ [11]. Here $L_z = 2\tilde{E}_z / (d\tilde{E}_z / dz)$ is the parallel length scale of the ponderomotive potential.

Thus, the neutral gas breakdown and initial ionization will be efficient when electrons will be trapped in the antenna RF potential wells for many periods and the amplitude of the antenna electric field will meet the boundary condition:

$$(\omega / e)(2m_e\varepsilon_i)^{1/2} \leq \tilde{E}_z(r) \leq 0.2 m_e\omega^2 L_z / e\,. \qquad (3)$$

After the first (gas local breakdown) phase of the RF discharge, as ω_{pe} becomes of the order of ω (it occurs at a very low density ~10^{12}–10^{14} m^{-3} in the frequency range 10 −100 MHz), plasma waves can start propagating in a relay-race regime governed by the antenna κ_z-spectrum, causing further space ionization of the neutral gas and plasma build-up in the torus (plasma phase). Because of the very low plasma temperature during the ionization phase (T_e~3–5 eV [6,10,12]), the RF power is expected to be dissipated mostly collisionally either directly or through conversion to ion Bernstein waves (IBW) if $\omega > \omega_{ci}$ or by conversion at the Alfvйn resonance if $\omega < \omega_{ci}$. Such a non-resonant coupling allows RF plasma production at any B_T.

3. EXPERIMENTAL SET-UP

The ICRF-DC experiments on reviewed tokamaks have been performed using the standard ICRF systems and under the following conditions:

- On TEXTOR (plasma major radius R_0=1.75 m, minor radius a≈0.46 m): 1 to 2 ICRF antennas (each consists of two poloidal current straps either solid or made of three parallel tubes) powered with $P_{RF/ant}$ ≈50–250 kW, f=32.5 MHz, pulse length τ_{RF}=0.2–1.0 s and *zero-* or π-phasing have been tested. ICRF discharges have been performed in pure toroidal magnetic field B_T=0.5–2.5 T in helium, deuterium and oxygen in the pressure range p≈1.0×10^{-3} Pa –1.5×10^{-1} Pa.

- On TORE SUPRA (R_0=2.38 m, a≈0.83 m): one double strap ICRF antenna was used in the following regime: $P_{RF/ant}$≈50–100 kW, f=47.9 MHz, τ_{RF}≤30.0 s, *zero*-phasing, no changes in hardware. The ICRF-DC experiments were performed in *He* or D_2 (p≈0.02–0.1 Pa) in a magnetic configuration with pure B_T=2.43–3.85 T and/or with additionally applied vertical magnetic field B_V ≤0.1 T.

- On AUG (R_0=1.65 m, horizontal a_h≈0.5 m and vertical a_v≈0.8 m minor radii): 1 to 4 double strap ICRF antennas were used with $P_{RF/ant}$≈3–120 kW, f_1=30.0 MHz, f_2=36.5 MHz, π-phasing. The ICRF system operated without any modifications in hardware. Multi-pulse (6× 300 ms) or long pulse (up to 4 s) ICRF discharges were performed in a magnetic configuration: B_T=1–2 T, B_V≤0.1 T in *He* or in a gas mixture (*He*+≤30%H_2) in the pressure range p=(1–8)×10^{-2} Pa.

- On JET (R_0=2.96 m, a_h≈1.25 m, a_v≈2.10 m): one ICRF antenna (array C with four poloidal current straps) was used with $P_{RF\text{-}tot}$ ≈130–245 kW, f≈34 MHz, π-phasing and τ_{RF}=0.5–4 s. Some modifications in the RF generator control system were done to manage operation in the RF plasma generation regime. Similar to the AUG case, ICRF discharges were generated in *He* and in a gas mixture (*He*+~20%H_2) in the pressure range p_{tot}=(1–8)×10^{-3} Pa and at B_T=1.85–2.45 T.

4. ICRF-DC CHARACTERIZATION

4.1. NEUTRAL GAS BREAKDOWN

To avoid deleterious effects of the neutral gas breakdown and arcing inside the antenna box, the frequency of RF generators and the RF voltage/power at antenna straps were reduced to technically available minimal values still meeting the requirements (3) for ICRF breakdown outside of the antenna box. As a result of the precautionary measures, reliable RF breakdown of the neutral gas and discharge initiation (ω≈4ω_{cHe+}=ω_{cH}) were possible in the machines over the whole parameter range covered (see Section 3). Figure 1 shows the transition from the RF breakdown phase to the ICRF discharge phase in JET. Here $\langle P_{RF/strap}\rangle$ and $\langle V_{RF/strap}\rangle$ are the RF power and the RF voltage in antenna vacuum transmission line, both averaged over four radiating straps. It is clearly seen that the gas breakdown occurs after some delay and shows up in a drop in the antenna RF voltage and in a burst in the H_α emission (measured far away from the antenna port).

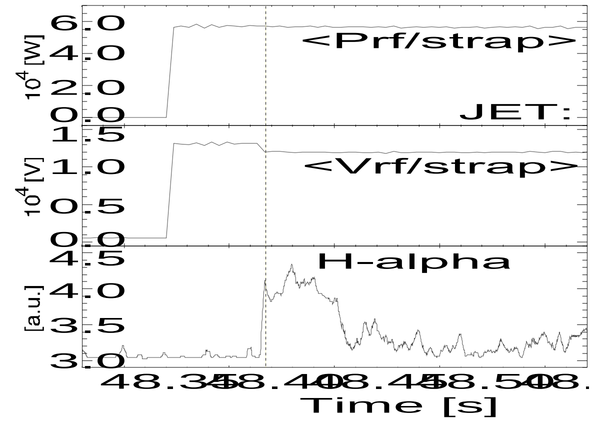

Fig.1. The transition from the neutral gas breakdown phase to the ICRF discharge phase in JET, after [10]

From the point of view of ICRF system operation, such a correlation is the sign of RF discharge initiation outside of the antenna box and subsequent plasma propagation along the magnetic field lines.

The pressure dependence of the neutral gas breakdown time (associated with the RF voltage drop and the occurrence of the initial peak in the H_α emission) is plotted in Fig.2 for RF discharges with similar RF power per strap (30–50 kW) and frequency (~30 MHz). A tendency towards an increase in breakdown time at low pressure is clearly seen. This results from the reduced collisionality and probability for an ionization event. At pressures higher than that shown in Fig.2 we expect a delay in breakdown to increase again due to increased collisionality and reduction in the electron kinetic energy. Therefore, a pressure range of p_{He}≈(2–6)×10^{-2} Pa appears as an optimal "pressure window" for ICRF discharge initiation at f~30 MHz.

Data from three tokamaks (TEXTOR, AUG and JET) were found in a good agreement, which might be an indication that the antenna RF voltage (the antenna-near $\tilde{E}_z$ electric field) plays a fundamental role in the neutral gas ICRF breakdown and that <u>the breakdown time is independent on the machine size</u>.

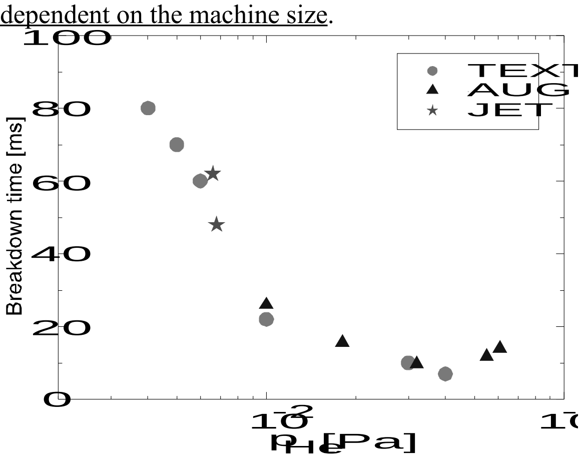

Fig.2. Pressure dependence of the RF breakdown time derived from the H_α emission analysis ($P_{RF/Ant.\ strap}$≈30–50 kW, f≈30 MHz, $\omega=4\omega_{cHe+}=2\omega_{cD}=\omega_{cH}$), after [10]

4.2. RF PLASMA CHARACTERISTICS

To find the range in B_T where the ICRF-DC initiation would be possible and reliable, the first set of discharges in TEXTOR were performed in a multi-pulse regime, while B_T was ramped down in time (Fig.3).

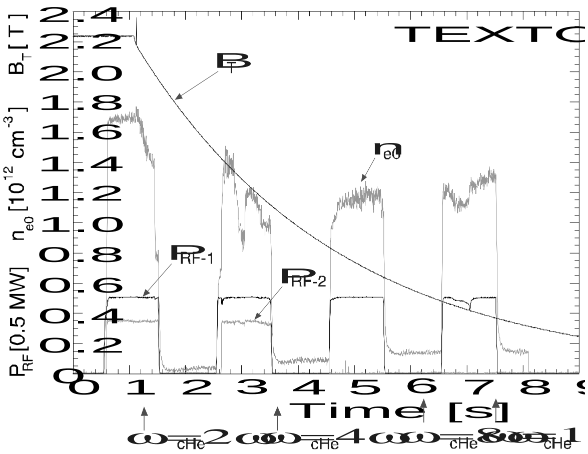

Fig.3. One of the first ICRF-DC experiments in TEXTOR: antennas A1 and A2 in π-phase, $f_1=f_2$=32.5 MHz, P_{RF-A1}=250 kW, P_{RF-A2}=170 kW, helium gas, $p_{He}\approx 1.5\times10^{-1}$ Pa

Both TEXTOR ICRF antennas were excited simultaneously (A1 and A2 in π-phasing). Helium plasmas with central line averaged density $\bar{n}_{e0}$ ≈(1.2–1.7) $\times10^{18}$ m^{-3} were easily produced in a wide range of B_T=0.36–2.24 T, starting with ~50 kW of RF generator power. At low B_T, the (line-averaged) density profile, deduced from signals of the 9-channel HCN-interferometer, was asymmetric with a large density gradient at the machine low field side (LFS). At high B_T, the density profile was broadly peaked mainly in the centre. A similar variation of the plasma profile was observed on TORE SUPRA [8]. The exterior line-integrated H_α emission measured in different sections of the torus vessel indicated that the distribution of ICRF plasmas in the toroidal direction was uniform. The electron temperature (deduced from spectroscopic and electric probe measurements) was in the range 10–20 eV, increasing in the low gas pressure case [4].

The antenna-plasma coupling efficiency was determined as a fraction of generator power radiated into the plasma [4]:

$$\eta = P_{RF-pl}/P_{RF-tot} = (R_{ant-tot} - R_{ant-vac})/R_{ant-tot}\ . \quad (4)$$

For the AUG antennas, the factor η was found between 50% (high B_T=2 T) and 75% (low B_T=1 T). This result was in agreement with the TEXTOR and TORE SUPRA data base [4,8] and in line with the fast wave (FW) propagation properties [8]. Unexpectedly low antenna coupling efficiency at JET (less than 25% according to a preliminary estimate) resulted in the antenna operation at RF voltages close to the upper limit and sporadic tripping occurred. This will be the subject of further investigations.

The CCD cameras are widely used to monitor the RF discharges in toroidal and poloidal directions. The CCD views from the non-circular tokamaks AUG and JET indicated that pure helium ICRF plasmas were toroidally uniform (like on circular machines) but poloidally located mostly at the LFS (ICRF antennas side) as shown on Figs.4a,5. The ECE radiation temperature data confirmed that RF plasmas extended radially in front of the AUG ICRF antennas by 15 cm only.

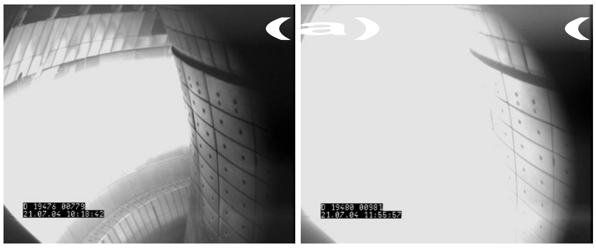

Fig.4. The CCD toroidal view of two AUG ICRF discharges #19476 in He (a) and #19480 in a gas mixture of H_2/He~30% (b) under the similar other conditions: P_{RF} ≈50 kW, f=30.0 MHz, B_T=2.4 T, p≈4×10^{-2} Pa

To improve the RF plasma homogeneity, which is necessary for efficient wall conditioning, several recipes have been tested on the divertor machines. The poloidal extent of the *He* plasmas on AUG could be increased by superposing an additional vertical magnetic field on B_T ($B_V \ll B_T$). On both, JET and AUG, the plasma extended radially over the vessel center towards the HFS when a gas mixture of helium and hydrogen (up to 30%) was injected (Figs.4b,5).

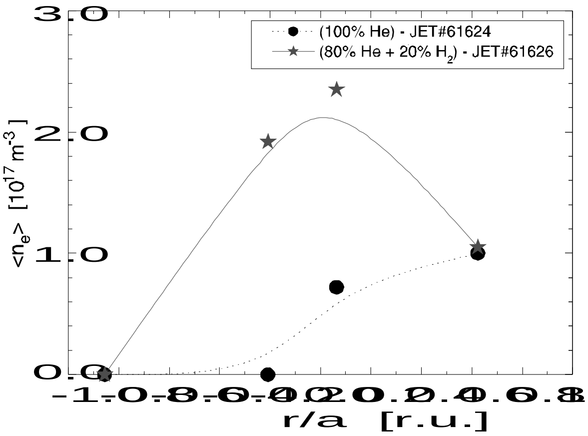

Fig.5. The line-averaged plasma density profiles for two JET ICRF discharges #61624 in He and #61626 in a gas mixture of H_2/He~20% under the similar other conditions: P_{RF}=230 kW, f≈34 MHz, B_T=2.45 T

The recent AUG experiments demonstrated that in the gas mixture case the plasma radial extension was proportional to the H_2 concentration and puff duration. Variation of the toroidal magnetic field and the frequency of RF generator revealed that better homogeneity of the ICRF-DC might be achieved in $(H+He)$-plasmas when the ICR layer $\omega=\omega_{cH}$ and the nearby FW-IBW mode conversion were shifted to the LFS. This effect has been predicted from the electron energy deposition profiles calculated with the 1D RF model of Ref. [13] for helium RF plasmas with variable H concentrations.

Analysis of the core atomic spectroscopy data showed appearance of the H_α, D_α and *HeI* (neutral) lines during the JET ICRF discharges. The impurity analysis of the VUV spectroscopy data indicated that the main impurity observed in JET ICRF discharges was *HeI*. Assuming an equilibrium (coronal) ionization balance, T_e can be approximately derived from the ionization stages observed. This evaluation resulted in T_e ~2−5 eV for shots at the gas pressure $p_{tot}\approx(2-6)\times10^{-3}$ Pa. <u>There was no evidence in the VUV spectrum of lines or bands of lines that could be due to metals [10].</u>

Analysis of the line-integrated density on both divertor machines ($\int n_e dl \leq 7\,10^{17}$ m^{-2}) showed that the RF plasma density was proportional to the injected RF power (a sign of weakly ionized plasma) and increased with the torus pressure. The ionization degree roughly estimated from the averaged density/pressure measurements was found to be rather low, $n_e/(n_e+n_0) < 0.1$.

All ICRF-DC experiments performed until now reported on the generation of high-energetic fluxes of H (with energies up to 60 keV) and of D atoms (up to 25 keV), which were detected by a neutral particle analyzer (NPA) [4,6-10]. Figure 6 shows typical H and D atoms spectra observed in two similar AUG ICRF discharges performed in different magnetic fields. The NPA viewing line passed roughly through plasma center and was oriented along the torus major radius in horizontal plane and vertically with 13 degrees upwards with respect to the horizontal plane.

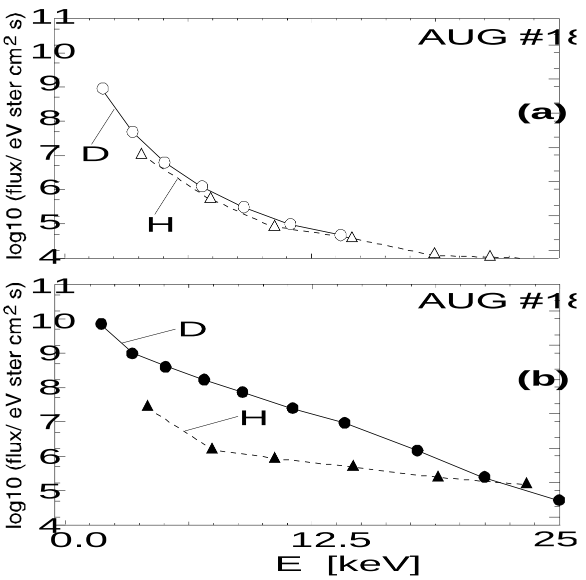

Fig.6. Hydrogen (dashed) and Deuterium (solid) atom spectra observed with NPA in the similar AUG ICRF discharges (P_{RF} ≈370 kW, p_{He}≈ 4.0×10^{-2} Pa) at:
(a) B_T=2.0 T and (b) B_T=1.0 T

At B_T=2.0 T (on-axis resonances $\omega=\omega_{cH}=2\omega_{cD}$), H and D atoms spectra have the same shape up to 14 keV (Fig.6a) with the similar averaged energy $\overline{E}_{\perp H} \approx \overline{E}_{\perp D} \approx$3.0 keV. On the contrary, for B_T=1.0 T (twice higher on-axis cyclotron harmonic resonances $\omega=2\omega_{cH}=4\omega_{cD}$) clear evidence of tail formation in distribution functions of H and D atoms was observed (Fig.6b) with higher averaged energy for hydrogen ($\overline{E}_{\perp H} \approx$5.0 keV, $\overline{E}_{\perp D} \approx$2.5 keV). This fact may be understood in terms of RF quasilinear diffusion: cyclotron harmonic heating tends to accelerate more the faster particles with tail formation at higher energy than fundamental heating [14]. More pronounced formation of the suprathermal tail at the fundamental resonance $\omega=\omega_{cH}$ was observed only in a low-pressure range p~3×10^{-3} Pa [7].

4.3. ICRF WALL CONDITIONING

The discharge conditioning is attributed to the removal of adsorbed gas species from the wall so that they may then be pumped out of the system. The adsorbed atoms may be removed by electronic excitation, chemical interaction and momentum/energy transfer [15]. For the latter mechanism, the rate of desorption increases with the impact energy of the ions and their masses [16]. ICRF discharges generate high-energetic fluxes of ions and neutrals due to presence of cyclotron mechanism (Fig.6) and may be considered promising for wall conditioning.

The wall conditioning effect could clearly be seen by an increase in the partial pressure of gases with different masses. The mass spectra of the residual gas recorded before and after the JET ICRF conditioning shot (#61631) were quite different indicating both, gas-into-vessel injection and wall conditioning effect (Fig.7).

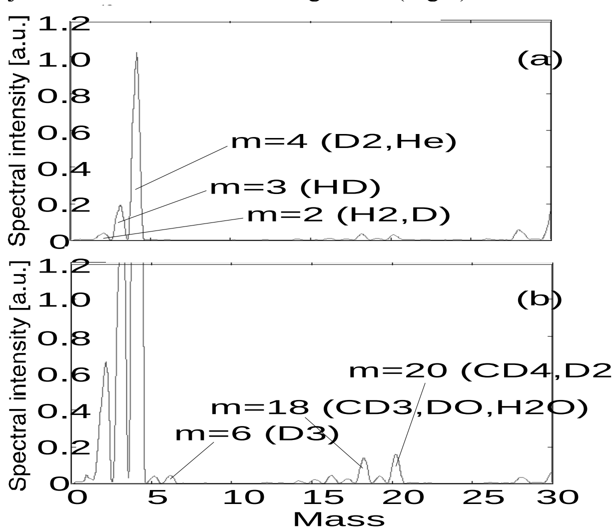

Fig.7. Mass-spectrum of the residual gas in the JET vessel before (a) and after (b) the ICRF conditioning shot #61631 (constant P_{RF-gen}≈230 kW, decaying B_T= 2.45−1.85 T and p_{tot}≈(7−1)×10^{-3} Pa), after [10]

More systematic studies of the wall conditioning efficiency were performed on limiter tokamaks TEXTOR [3-5] and TORE SUPRA [6,7]. The effect of wall conditioning is clearly seen on Fig.8. Here, the integral of the hydrogen pressure that represents the amount of the desorbed gas coming from the wall after the five successive TEXTOR ICRF-DC pulses is shown. The total amount of the desorbed hydrogen was of the order of ~6.4×10^{20} H-atoms which corresponds to ~1 monolayer of the whole inner wall area [3]. Later, the ICRF-DC efficiency in helium was compared with that of G-DC on TORE SUPRA [6] and of ECRF-DC on TEXTOR [5]. The hydrogen removal rate in the ICRF-DC ($\omega\approx4\omega_{cHe+}=\omega_{cH}$) was found to be about 10 times higher than in the typical G-DC and about 20 times higher than in the ECRF-DC ($\omega\approx2\omega_{ce}$) produced by a focused microwave beam. Both the better homogeneity of the ICRF discharge and the generation of energetic neutrals bombarding the wall could contribute in the achieved results.

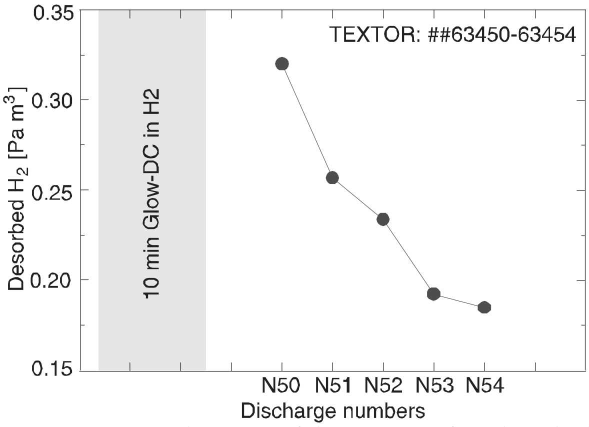

Fig.8. Successive decrease of the amount of H_2 desorbed from a H_2 preloaded first wall due to ICRF wall conditioning in He, after [3]

CONCLUSIONS

ICRF discharges with improved homogeneity and high conditioning efficiency were demonstrated in a wide range of machine parameters using the present-day ICRF antennas. Scaling of the ICRF-DC with the machine size was successfully tested on European limiter and divertor tokamaks including the largest one – JET. Extrapolation of the ICRF-DC parameters achieved at a low power-per-density case [7] ($P_{RF}\approx$ 100 kW, $p\approx2.0\times10^{-2}$ Pa) to the ITER size (R_0=6.2 m, $a_h\approx2.0$ m, $a_v\approx3.72$ m), assuming the worst case of linear dependence of the plasma confinement time on size [4], will give us an upper estimate of the order of ~1.5–3.0 MW for the RF power delivered to the launcher system (24 strap antenna array) at f=40.0 MHz and B_T<3.5 T ($\omega>\omega_{cH}$) or B_T>4.0 T ($\omega<\omega_{cH}$). The present analysis shows a high potential of the ICRF discharges for wall conditioning in the fusion devises. However, more systematic studies on divertor tokamaks are necessary to optimize the ICRF discharge and quantify more the conditioning effect.

ACKNOWLEDGEMENTS

This work has been performed under the European Fusion Development Agreement. The authors gratefully thank Dr. J. Pamйla and Dr. O. Gruber for their encouragement and stimulating support.

REFERENCES

1.O.M. Shvets, et al. RF production and heating of plasma in URAGAN-3 torsatron// *Proc. of the 4th Int. Symp. Heating in Toroidal Plasmas, Roma, 1984.*/ ENEA, Frascati, 1984, Vol.1, pp.513-528.
2.N.I. Nazarov, et al. Use of RF plasma to clean the surfaces in the URAGAN-3 torsatron// *Sov. J. Plasma Phys.* (13), 1987, N12, pp.871-873.
3.H.G. Esser, et al. ICRF wall conditioning at TEXTOR-94 in the presence of a 2.25 T magnetic field// *Journal of Nuclear Materials* (241-243), 1997, pp.861-866.
4.A. Lyssoivan, et al. ICRF plasma production and application to start-up and wall conditioning// Final Report on ITER Design Task D350.2. Brussels, 1998, LPP-ERM/KMS Laboratory Report N114.
5.E. Gauthier, et al. ECR and ICRF conditioning discharges comparison in TEXTOR-94// *Proc. of the 28th EPS Conf. Contr. Fusion and Plasma Phys., Madeira, 2001.*/ Paper P5.094.
6.E. Gauthier, et al. Wall conditioning technique development in TORE SUPRA with permanent magnetic field by ICRF wave injection// *Journal of Nuclear Materials* (241-243), 1997, pp.533-558.
7.E. de la Cal and E, Gauthier. First wall cleaning and isotope control studies by D_2 ICRF conditioning in TORE SUPRA with a permanent magnetic field// *Plasma Phys. Control. Fusion* (39), 1997, pp.1083-1099.
8.A. Lyssoivan, et al. ICRF plasma production in TORE SUPRA: analysis of antenna coupling and plasma properties// *Proc. of the 26th EPS Conf. Contr. Fusion and Plasma Phys., Maastricht, 1999.*/ ECA, 1999, Vol.23J, pp.737-740.
9.J.K. Xie, et al. RF wall conditioning – a new technique for future large superconducting tokamak// *Journal of Nuclear Materials* (290-293), 2001, pp.1155-1159.
10.A. Lyssoivan, et al. Development of ICRF wall conditioning technique on divertor-type tokamaks ASDEX Upgrade and JET// *Proc. of the 16th Int. Conf. Plasma Surface Interactions, Portland, 2004.*/ Paper P1-36, to be published in *Journal of Nuclear Materials.*
11.M.D. Carter, et al. Plasma production using radiofrequency fields near or below the ion cyclotron range of frequencies// *Nuclear Fusion* (30), 1990, N4, pp.723-730.
12.A.I. Lyssoivan, et al. Analysis of ICRF ($\omega\le\omega_{ci}$) plasma production in large-scale tokamaks// *Nuclear Fusion* (32), 1992, N8, pp.1361-1372.
13.D. Van Eester and R. Koch. A variational principle for studying fast-wave mode conversion // *Plasma Phys. Control. Fusion* (40), 1998, pp.1949-1976.
14.R. Koch. The ion cyclotron, lower hybrid and Afvйn wave heating methods// *Transactions of Fusion Science and Technology* (45), 2004, N2T, pp.203-210.
15.P.C. Stangeby and G.M. McCracken. Plasma boundary phenomena in tokamaks// *Nuclear Fusion* (30), 1990, N7, pp.1225-1379.
16.J. Winter. Wall conditioning in fusion devices and its influence on plasma performance/ *Plasma Phys. Control. Fusion* (38), 1996, pp.1503-1542.

РАЗРАБОТКА МЕТОДОВ ПОДГОТОВКИ ВАКУУМНОЙ СТЕНКИ ИТЕР'а С ПОМОЩЬЮ ВЧ В ОБЛАСТИ ИЦР ЧАСТОТ НА ЕВРОПЕЙСКИХ ТОКАМАКАХ

А.Лысоиван, Р.Коч, Д.Ван Эстер, М. Вервьер, Р.Вейнантс, Х.Г. Ессер, В.Филлипс, Е. Готье, Д.А.Хартманн, Ж.-М. Нотрдам, В. Бобков, Ф.Браун, И.Монахов, А.Вальден

В будущих термоядерных установках с сверхпроводящими магнитными системами масштаба ИТЕРа присутствие постоянного сильного магнитного поля будет препятствовать использованию обычных тлеющих разрядов для подготовки вакуумных стенок между разрядами. Поэтому только разряды, работающие при сильном магнитном поле, могут быть использованы для этих целей. ВЧ разряды в области частот ИЦР обладают большим потенциалом для решения этой проблемы. В настоящей работе представлен обзор новых ВЧ ИЦР техник подготовки стенок , развитых на токамаках с лимитером TEXTOR и TORE SUPRA и результаты первых испытаний на токамаках с дивертором ASDEX UPGRADE и JET.

РОЗРОБКА МЕТОДІВ ПІДГОТОВКИ ВАКУУМНОЇ СТІНКИ ИТЕР'а ЗА ДОПОМОГОЮ ВЧ В ОБЛАСТІ ІЦР ЧАСТОТ НА ЄВРОПЕЙСЬКИХ ТОКАМАКАХ

А.Лисойван, Р.Коч, Д.Ван Естер, М. Вервьєр, Р.Вейнантс, Х.Г. Ессер, В.Филлипс, Е. Готьє, Д.А.Хартманн, Ж.-М. Нотрдам, В. Бобков, Ф.Браун, И.Ченців, А.Вальден

У майбутніх термоядерних установках зі надпровідними магнітними системами масштабу ИТЕРа присутність постійного сильного магнітного поля буде перешкоджати використанню звичайних тліючих розрядів для підготовки вакуумних стінок між розрядами. Тому тільки розряди, що працюють при сильному магнітному полі, можуть бути використані для цих цілей. ВЧ розряди в області частот ІЦР мають великий потенціал для рішення цієї проблеми. У даній роботі представлений огляд нових ВЧ ІЦР технік підготовки стінок, розвитих на токамаках з лімітером TEXTOR і TORE SUPRA і результати перших іспитів на токамаках з дивертором ASDEX UPGRADE і JET.